



Cite this: *RSC Adv.*, 2019, 9, 37148

# Remote loading of curcumin-in-modified $\beta$ -cyclodextrins into liposomes using a transmembrane pH gradient†

Fadwa Odeh,<sup>‡\*a</sup> Hamdi Nsairat,<sup>‡a</sup> Walhan Alshaer,<sup>‡\*b</sup> Shrouq Alsotari,<sup>b</sup> Rula Buqaien,<sup>b</sup> Said Ismail,<sup>cd</sup> Abdalla Awidi<sup>bc</sup> and Abeer Al Bawab<sup>ae</sup>

Curcumin (CRM) is a natural polyphenol with antioxidative, anti-inflammatory, and anticancer therapeutic properties. However, CRM therapeutic potential is limited by low water solubility and bioavailability. Intraliposomal remote loading describes the retention of drugs in liposome cores in response to transmembrane pH gradient. The current study describes for the first time the remote loading of CRM into liposomes using secondary (E- $\beta$ CD) and tertiary (D- $\beta$ CD) amino-modified  $\beta$ -cyclodextrins ( $\beta$ CDs) as carriers and solubilizers.  $\beta$ CDs were chemically modified to prepare the ionizable weak base functional group followed by forming a guest-host complex of CRM in the modified  $\beta$ CDs hydrophobic cavities via a solvent evaporation encapsulation technique. These complexes were then actively loaded into preformed liposomes, composed of DPPC/cholesterol (65/35 molar ratio) via pH gradient. The formation of CRM- $\beta$ CDs inclusion complexes was characterized using UV-Vis spectroscopy, thermal analysis, and NMR spectroscopy. The complex stoichiometric ratio was determined to be 1 : 1 of CRM- $\beta$ CDs based on Job's plot which was also confirmed by the modified Benesi-Hildebrand equation with increasing probability of forming the 1 : 2 ratio of CRM- $\beta$ CDs. The apparent formation constants ( $K_f$ ) of 51.6, 100.9 and 55.4  $\text{mM}^{-2}$  were determined for CRM- $\beta$ CD, CRM-E- $\beta$ CD, and CRM-D- $\beta$ CD complexes, respectively. Liposome size, charge and polydispersity index indicate the presence of a homogeneous population before and after active loading. The encapsulation efficiencies of CRM- $\beta$ CD complexes into pH gradient preformed liposomes were 16.5, 51.1, and 41.7 for CRM- $\beta$ CD, CRM-E- $\beta$ CD, and CRM-D- $\beta$ CD, respectively, showing more than 5 fold increase compared to normal liposomes. The current study provides a novel remote loading approach utilizing chemically modified cyclodextrins to incorporate hydrophobic drugs into liposomes.

Received 18th September 2019  
Accepted 2nd November 2019

DOI: 10.1039/c9ra07560g

rsc.li/rsc-advances

## 1. Introduction

The poor aqueous solubility of hydrophobic drugs is limiting their therapeutic applications in the clinic. Many clinically effective drugs are hydrophobic and suffer from low water solubility and bioavailability.<sup>1</sup> Therefore, different strategies have been developed to overcome these limitations thereby improving therapeutic potency. One important strategy is the incorporation of hydrophobic drugs into carriers such as

cyclodextrins and nanoparticles to enhance their solubility and bioavailability.<sup>2,3</sup> Liposomes, consist of one or more lipid bilayers enclosing an aqueous core, are considered as one of the most successful drug delivery systems due to their biocompatibility, stability, easy to synthesize and high drug loading efficiency.<sup>4,5</sup> Liposomal drug loading can be achieved by either passive or active methods.<sup>6</sup> Liposomal passive loading is performed during the formation of the lipid bilayer vesicles. This approach can encapsulate the hydrophilic drug in the liposomes aqueous core, while water-insoluble drugs will accumulate in the small-sized hydrophobic lipid bilayer (~5 nm thickness).<sup>6-9</sup> However, the passive loading of hydrophobic drugs into the bilayer of liposomes is limited by bilayer destabilization, high lipid/drug ratio, and rapid drug release.<sup>10</sup> Therefore, methods to solubilize hydrophobic drugs such as complexation with cyclodextrins (drug-in-cyclodextrins) were successfully applied and permitted the loading of hydrophobic molecules into the liposomes aqueous core, hence forming drug-in-cyclodextrins-in-liposomes delivery system.<sup>11</sup> Cyclodextrins are truncated cone shape macrocyclic oligosaccharides

<sup>a</sup>Department of Chemistry, The University of Jordan, Amman 11942, Jordan. E-mail: f.odeh@ju.edu.jo; Tel: +962 6 5355000 ext. 22152; +962 792950409

<sup>b</sup>Cell Therapy Center, The University of Jordan, Amman 11942, Jordan. E-mail: walhan.alshaer@ju.edu.jo; Tel: +962 6 5355000 ext. 23960; +962 790823678

<sup>c</sup>Faculty of Medicine, The University of Jordan, Amman, Jordan

<sup>d</sup>Qatar Genome Project, Qatar Foundation, Doha, Qatar

<sup>e</sup>HMCSSR, The University of Jordan, Amman, Jordan

† Electronic supplementary information (ESI) available. See DOI: 10.1039/c9ra07560g

‡ Authors contributed equally to this work.



consisting of six, seven and eight glucopyranose units for  $\alpha$ ,  $\beta$  and  $\gamma$ -cyclodextrins, respectively. Structural studies have revealed that cyclodextrins have a hydrophobic central cavity and a hydrophilic outer surface.<sup>12,13</sup> Therefore, cyclodextrins have the ability to form complexes with specific water insoluble drug molecules *via* physical interactions in their hydrophobic cavities (guest–host interaction). These characteristics make them invaluable in the fields of pharmaceuticals and drug delivery.<sup>14,15</sup> Moreover, the hydroxyl groups of cyclodextrins are chemically reactive and can be modified with different functional groups that can improve pharmaceutical applications.<sup>16,17</sup>

Active or remote loading has been developed to ensure high intraliposomal drug concentrations and minimal loss of precious chemotherapeutic agents.<sup>18</sup> Remote loading can be achieved through loading drug molecules into preformed liposomes using pH gradient and/or ionic potential differences across liposomal membranes.<sup>7,10</sup> There are two main factors that direct the success of intraliposomal active loading, (i) the water solubility of the drug, and (ii) the presence of ionizable functional group in its structure which can facilitate active loading and accumulation of drugs inside liposomes.<sup>17,19</sup>

Curcumin (CRM) (Fig. S1†), bis(4-hydroxy-3-methoxyphenyl)-1,6-diene-3,5-dione, is a polyphenol molecule derived from the rhizome of the plant *Curcuma longa*. Currently, CRM has important attention in medicine for the wide range of its pharmacological applications such as anti-inflammation, anti-microbial, anti-oxidant, anti-parasitic, anti-mutagenic and anti-cancer.<sup>20,21</sup> CRM can be a good candidate for active loading into liposomes. However, CRM is missing the requirements for liposomal active loading, including its low solubility in aqueous solution ( $\approx 20 \mu\text{g mL}^{-1}$ ) and not bearing an ionizable functional group.<sup>17</sup> Moreover, applying chemical modifications to this natural active compound can alter its biological and chemical properties. Since incorporating drug-cyclodextrin complexes into liposomes were limited to passive loading,<sup>3,8,22</sup> modified cyclodextrins, bearing ionizable groups (Fig. S2†), may act as a promising carrier to actively load water-insoluble drugs in liposomes core, avoiding the drug chemical modification risk.<sup>17,23</sup> In the current work, we suggest a method for remote loading of CRM hydrophobic molecule into the aqueous core of liposomes through chemically modified  $\beta$ -cyclodextrins ( $\beta$ CDs) as carriers. In order to do so, we synthesized and characterized newly modified  $\beta$ CDs with weak bases as ionizable functional groups. Then, CRM was complexed with the modified  $\beta$ CDs and the resulting CRM-in- $\beta$ CDs inclusion complexes were characterized by thermal analysis, spectroscopic proton nuclear magnetic resonance (<sup>1</sup>H-NMR) and UV-visible spectrophotometric techniques. Finally, the ability of the modified  $\beta$ CDs to complex and remote loading of CRM into the core of liposomes was assessed using transmembrane pH gradient method.

## 2. Materials and methods

### 2.1. Chemicals

$\beta$ -Cyclodextrin ( $\beta$ CD), curcumin, bis(4-hydroxy-3-methoxyphenyl)-1,6-diene-3,5-dione (CRM) and *p*-toluenesulfonyl chloride (TsCl) were purchased from Sigma (St. Louis,

MO, USA). 1-Ethanol-2-amine (ethanolamine) and *N,N*-diethylamine (diethyl amine) were purchased from TEDIA (Fairfield, OH, USA). 1,2-Dipalmitoyl-*sn*-glycero-3-phosphocholine (DPPC) and cholesterol (CHOL) were obtained from Avanti Polar Lipids, Inc. (Alabaster, Alabama, USA). Phosphate buffer saline (PBS) and [4-(2-hydroxyethyl)-piperazino]-ethanesulfonic acid (HEPES) were obtained from LONZA® (USA). Deuterated dimethylsulfoxide ( $d_6$ -DMSO) (99.9% atom) was used for NMR analysis and was purchased from Aldrich (USA). Vinytec K was purchased from Aldrich, USA. Uranyl acetate reagent from Electron Microscopy Science (USA). Acetone, methanol, ethanol, acetonitrile, and 1-propanol were obtained from carbon group (England). All other chemicals and solvents were of analytical grade. All reagents and chemicals were used without further treatment.

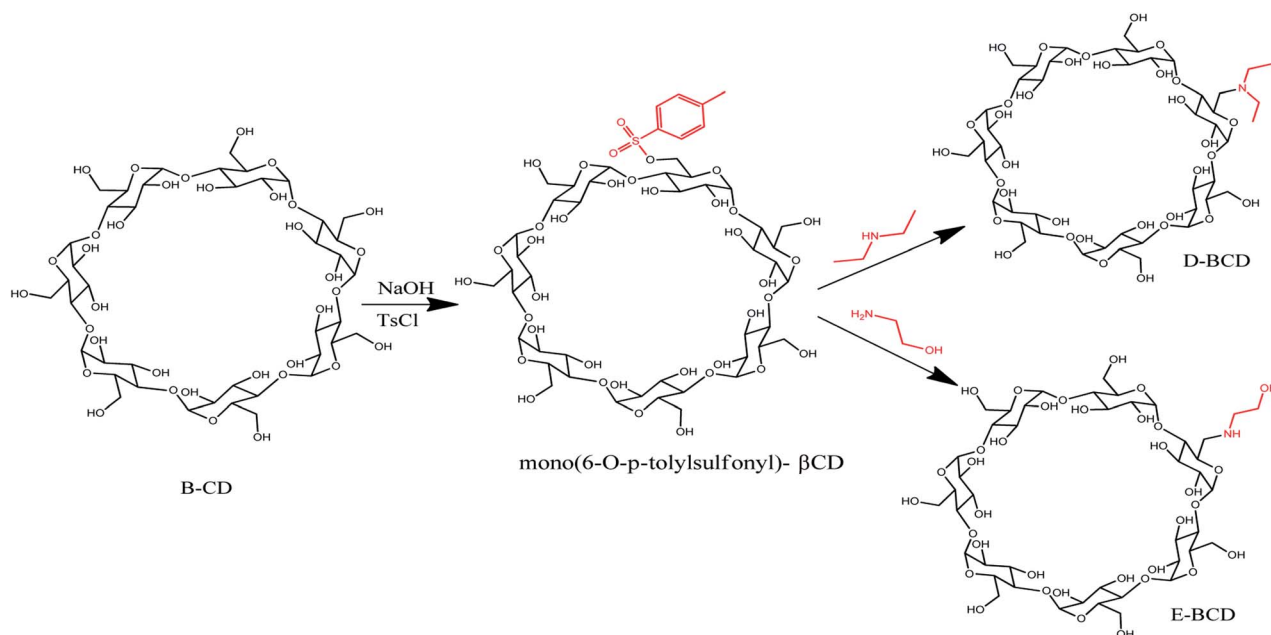
### 2.2. Synthesis of mono amino-modified $\beta$ CDs

The amino-modified  $\beta$ CDs, mono-6-deoxy 1-ethanol-2-amine- $\beta$ CD (E- $\beta$ CD) and mono-6-deoxy-*N,N*-diethylamine- $\beta$ CD (D- $\beta$ CD) were synthesized as illustrated in Scheme 1. Firstly, mono(6-*O*-*p*-tolylsulfonyl)- $\beta$ CD, 6-OTs- $\beta$ CD was synthesized by tosylation of  $\beta$ CD with *p*-toluenesulfonyl chloride (TsCl) in basic aqueous solution according to literature procedure with minor modifications,<sup>24</sup> where  $\beta$ CD (1.477 g, 1.3 mmol) and TsCl (0.429 g, 2.25 mmol) was dissolved in 35 mL of deionized water and stirred at room temperature for 3 h. Thereafter, sodium hydroxide, NaOH (0.60 g, 15 mmol) in 7 mL of deionized water was added and the mixture was stirred for 10 min. Unreacted TsCl was removed by filtration through a grade 4 sintered glass funnel. The filtrate was brought to pH  $\sim 7.5$  by the addition of  $\text{NH}_4\text{Cl}$  (1.3 g), then refrigerated overnight at 4 °C. The resulting white precipitate was recovered by filtration, and dried for 24 h at 80 °C. A pure white solid was obtained (47.52% yield).

The amino-modified  $\beta$ CDs, E- $\beta$ CD and D- $\beta$ CD, were synthesized by nucleophilic substitution of 6-OTs- $\beta$ CD with an excess of the corresponding aliphatic amines, 1-ethanol-2-amine (ethanolamine) and *N,N*-diethylamine (diethyl amine). A solution of 6-OTs- $\beta$ CD (0.30 g, 0.235 mmol) in an excess ethanol amine (17.625 mmol, 1.064 mL) was stirred at 70 °C for 18.0 h, then cooled to room temperature. Distilled water (1 mL) was added to dilute the mixture, the resultant solution was poured into a mixture of acetone (10 mL) and ethanol (10 mL) slowly, forming white precipitate immediately. The white precipitate was collected by suction filtration and recrystallized three times in hot water ( $3 \times 1 \text{ mL}$ ), 0.2217 g of E- $\beta$ CD was produced (80.01% yield).<sup>25</sup>

17.625 mmol, 1.822 mL excess amount of diethyl amine was added to 0.30 g, 0.235 mmol of 6-OTs- $\beta$ CD, the solution stirred at 40–50 °C for four days. The excess diethylamine was removed under vacuum. The product (D- $\beta$ CD) was obtained by recrystallization from hot water ( $3 \times 1 \text{ mL}$ ), yielding 0.2 g (71.55%) as a white crystal.

These products were characterized by proton nuclear magnetic resonance (<sup>1</sup>H-NMR) analysis using Bruker Avance III 500 MHz instrument (Bruker BioSpin, Switzerland) and by high-resolution mass spectroscopy with electrospray ionization method operating HRMS (ESI) using ESI-apex-IV Bruker Mass spectrometry.



Scheme 1 Schematic synthesis of the modified β-cyclodextrin (E-β-CD and D-β-CD).

### 2.3. Preparation of encapsulated complexes

The preparation of inclusion complexes of CRM with different βCDs was performed *via* solvent evaporation encapsulation technique.<sup>26</sup> A 1 : 2 drug to cyclodextrin ratio (0.044 mmol, 16.8 mg) of CRM dissolved in methanol (nearly saturated ~1 mL) and appropriate cyclodextrin (0.022 mmol, 25, 26.2 and 26.1 mg for βCD, E-βCD, and D-βCD, respectively) dissolved in deionized water (~2 mL). The methanolic solution of the CRM was then added dropwise into the cyclodextrin solution in 5 mL round bottom flask. This solution was then mixed by shaking, without a cap to evaporate the methanol, at 300 rpm and 40 °C for 36 h. The complex solution was used after filtration, to remove the particulate matter, for spectrophotometric and active loading investigation or dried in the fume hood overnight and completely dried using vacuum oven at 35 °C for 2 h for further characterization.<sup>17,21</sup>

### 2.4. Spectrophotometric studies

Spectroscopic studies were carried out to determine the absorption spectrum, stoichiometry, and formation constant of the inclusion complexes. Absorption spectra were recorded in the range of 300 to 500 nm using Nanodrop 2000 UV-Vis spectrophotometer (Wilmington, DE, USA).<sup>27</sup>

**2.4.1 Absorption spectra.** The absorption spectra and the effect of increasing concentration of βCDs on the absorption spectra of CRM were recorded for different inclusion complexes with a constant concentration of CRM and increasing concentration of βCDs from 1 to 3 molar ratio.

**2.4.2 Determination of the complexation stoichiometry.** Continuous variation method (Job's method) was used to determine the complexation stoichiometry.<sup>28,29</sup> The experiments were performed using solutions of equimolar concentrations of the CRM and βCDs. The samples were prepared by mixing

different volumes of these two solutions so that the total concentration remains constant and the molar fraction of the drug,  $X$  varies in the range from 0–1. The absorbance differences, in presence of βCDs with respect to the value for the free CRM, were recorded at different molar ratios at maximum wavelength ( $\lambda_{\max}$ ) = 420 nm.<sup>30</sup> The variation of the absorbance differences ( $\Delta\text{Abs}$ ) multiplied by CRM concentration is plotted *versus* CRM mole fraction ( $X$ ). The value of  $X$  for which the plot presents the maximum deviation gives the stoichiometry of the inclusion complex ( $X = 0.5$  for 1 : 1 or 2 : 2 ratio complexes;  $X = 0.33$  for 1 : 2 ratio complexes).<sup>31</sup>

**2.4.3. Determination of formation constants.** The binding constant of drug-cyclodextrin inclusion complex was determined by Benesi-Hildebrand equation.<sup>28</sup> The concentration of CRM was kept constant and βCD and the modified βCDs concentration was varied from 1–3.5 molar ratio. Eqn (1) used for 1 : 1 complexation and eqn (2) for 1 : 2 complexation.<sup>32</sup>

$$\frac{1}{A - A^0} = \frac{1}{A' - A^0} + \frac{1}{K(A' - A)[\beta\text{CD}]} \quad (1)$$

$$\frac{1}{A - A^0} = \frac{1}{A' - A^0} + \frac{1}{K(A' - A)[\beta\text{CD}]^2} \quad (2)$$

where  $A^0$  is absorbance of the guest without βCD,  $A$  is the absorbance with a particular concentration of βCD,  $A'$  is the absorbance at the maximum concentration of βCD. The formation constant ( $K$ ) is calculated from the Benesi-Hildebrand equation,<sup>33</sup> after plotting  $(1/A - A^0)$  against  $(1/[\beta\text{CD}])$  or  $(1/[\beta\text{CD}]^2)$ :

$$\text{Formation constant } (K) = \frac{1/(A^0 - A)}{1/(A' - A^0)} \quad (3)$$

## 2.5. Differential scanning calorimetry (DSC) and thermogravimetric analysis (TGA)

The complexed nanoparticles were analyzed on Netzsch DSC 204 F1 instrument (Germany). The DSC patterns of the samples were obtained from 20 °C to 300 °C at a heating rate of 10 °C min<sup>-1</sup>, under a constant flow (100 mL min<sup>-1</sup>) of nitrogen gas. The samples weights were in the range of 3–6 mg.

The TGA analysis was performed on Mettler Toledo Instrument (TGA/DSC 2, Switzerland) from 25 °C to 500 °C with a heating rate of 10 °C min<sup>-1</sup>. Alumina (aluminum oxide, ALU) crucibles, holding 1–2 mg of each sample, were used.

## 2.6. <sup>1</sup>H-NMR spectroscopy

All NMR spectra were performed in d<sub>6</sub>-DMSO (99.0% atom, Across Organics, USA) using Bruker Avance III 500 MHz instrument (Bruker BioSpin, Switzerland) with a Broadband Observe (BBO) probe equipped with z-gradient and the temperature was controlled using a variable temperature unit (VTU) and held constant at 300 K. Chemical shift in parts per million (ppm) were referenced to tetramethylsilane (TMS) as an internal reference. Data processing and analysis of the data were performed with topspin framework (Bruker Biospin GmbH, Version 3.6.0).

## 2.7. Mass spectrometry

High-resolution mass spectra (HRMS) were acquired (in positive or negative mode) using electrospray ion trap (ESI) technique by collision-induced dissociation on a Bruker APEX-4 (7 Tesla) instrument. The samples were infused using a syringe pump at a flow rate of 2 μL min<sup>-1</sup>.

## 2.8. Liposomes preparation and active loading

**2.8.1. Preparation of transmembrane pH gradient conventional liposomes.** Liposomes were prepared using the conventional thin-film hydration technique.<sup>34,35</sup> Briefly, 4.78 mg of DPPC, 1.36 mg cholesterol (65 : 35 molar ratio) were dissolved in 3–4 mL chloroform, which was then evaporated under reduced pressure, down to 100 mbar (IKA RV 05 Basic Rotary Evaporator combined with VacuuBrand CVC2000, Germany) at 20 rpm and 35 °C water bath until a dried, homogeneous thin film was obtained. The film was then hydrated with 2 mL of 300 mM citrate buffer, pH 4.0 at ~50 °C for 30–60 min with vigorous vortexing every 2–3 min.<sup>17</sup> The vesicle suspension was extruded successively through a polycarbonate membrane (100 nm, Whatman®) using Mini-Extruder (Avanti Polar Lipids, Inc. USA) at 50 °C for 13 times to obtain the final liposomes with low polydispersity and the desired size, which were stored at 4 °C for further use. The transmembrane pH gradient was achieved by re-dispersing the liposomes pellets, after 15 300 rpm centrifugation at 4 °C for 1.5 h, with an external 20 mM (pH = 10.5) HEPES buffer.

**2.8.2. Remote loading protocol into liposomes.** A 200 μL of CRM: βCD complex (0.17 mM) incubated in 400 μL (5.0 mM) of freshly prepared pH gradient liposome for 1.0 h at 65 °C.<sup>17</sup> The suspension was left to cool at room temperature and then

centrifuged at 9000 rpm, 4 °C for 1.0 h to remove CRM: βCD complex that had not been loaded into the liposomes. The liposomes pellets were then disrupted with 500 μL methanol by 3 min vortexing followed by 15 300 rpm and 4 °C centrifugation for 15 min. The supernatant was measured on UV-Vis spectrophotometer at 420 nm for the loaded CRM: βCD complexes.<sup>17,36</sup>

**2.8.3. Nanoparticle size and zeta potential.** The average size, charge and polydispersity index (PDI) for liposomes before and after active loading were measured by dynamic light scattering experiments on a Zetasizer, Nano-ZS (Malvern Instruments Ltd., Malvern, UK). Liposomal samples were diluted with deionized water in order to yield an appropriate counting rate. All samples were placed into the specimen holder of a Zeta-sizer for 60 s prior to the measurement in order to allow room temperature equilibrium.<sup>36</sup>

**2.8.4. Transmission electron microscopy (TEM).** TEM analysis of different liposomes were performed using negative staining method.<sup>37</sup> First, 200 mesh formvar copper grids (SPI supplies, USA) were coated with carbon under low vacuum Leica EM ACE200 glow discharge coating system (Leica, Austria). Then, the carbon-coated grids were further coated with 1.5% vinyl K solution in chloroform. A drop of deionized water-diluted liposomes suspension was placed on the 200 mesh formvar copper grid followed by air-drying. The loaded grids then stained with 3% (v/v) of aqueous solution of uranyl acetate for 20 min at room temperature. After incubation, grids were washed with distilled water and dried at room temperature before imaging with Versa 3D (FEI, Netherlands) TEM operating system at an acceleration voltage of 30 kV.<sup>11</sup>

**2.8.5. Liposomes encapsulation efficiency (EE%).** The encapsulation efficiency of CRM: βCD complex into liposomes was expressed as the percent of drug complex encapsulated inside liposomes and calculated using the following equation:<sup>37</sup>

$$\text{Encapsulation efficiency (EE\%)} = \frac{[\text{Entrapped CRM complex}]}{[\text{Total CRM complex}]} \times 100 \quad (4)$$

# 3. Results and discussion

## 3.1. Characterization of modified β-cyclodextrins

The formation of mono-6-deoxy-6-(*p*-tolylsulfonyl)-β-cyclodextrin (6-OTs-βCD) (Fig. S3†) was confirmed using <sup>1</sup>H-NMR and mass spectrometry. HRMS (ESI) on the negative mode ([M – H]<sup>-</sup>) confirmed 6-OTs-βCD (C<sub>49</sub>H<sub>75</sub>O<sub>37</sub>S) synthesis, where the calculated and the found values are 1287.37134 and 1287.29928, respectively, in addition to the isotope peaks (Fig. S4†).

Compared to <sup>1</sup>H-NMR spectrum of βCD (Fig. S5†), new doublet peaks of the proton signal appeared around 7.45 and 7.77 ppm, which belongs to the C9-H and C8-H proton of the aromatic ring, respectively (Fig. S6†). A singlet peak arises at 2.45 ppm for the *para*-methyl group (C11-3H) of the aromatic ring.

<sup>1</sup>H NMR (d<sub>6</sub>-DMSO, δ, ppm) for 6-OTs-βCD: 2.45 (s, 3H, –CH<sub>3</sub>), 3.23–3.38 (m, 14H, H-2,4), 3.60–3.75 (m, 28H, H-3,5,6), 4.79 (d, 2H, H-1), 4.86 (t, 5H, H-1), 5.74 (m, 14H, OH-2,3), 7.45 (d, 2H, H-9), 7.77 (d, 2H, H-8).



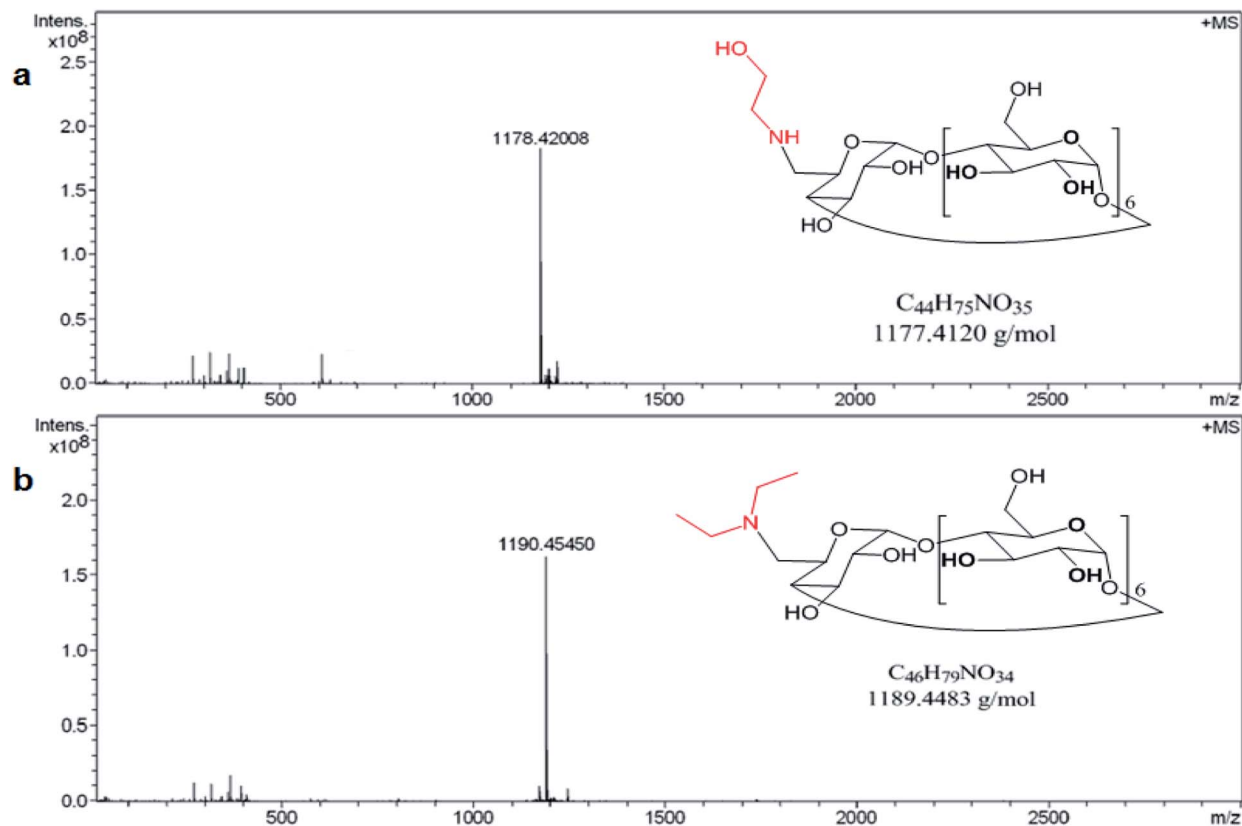


Fig. 1 Mass spectrum of (a) E- $\beta$ CD and (b) D- $\beta$ CD one the positive mode.

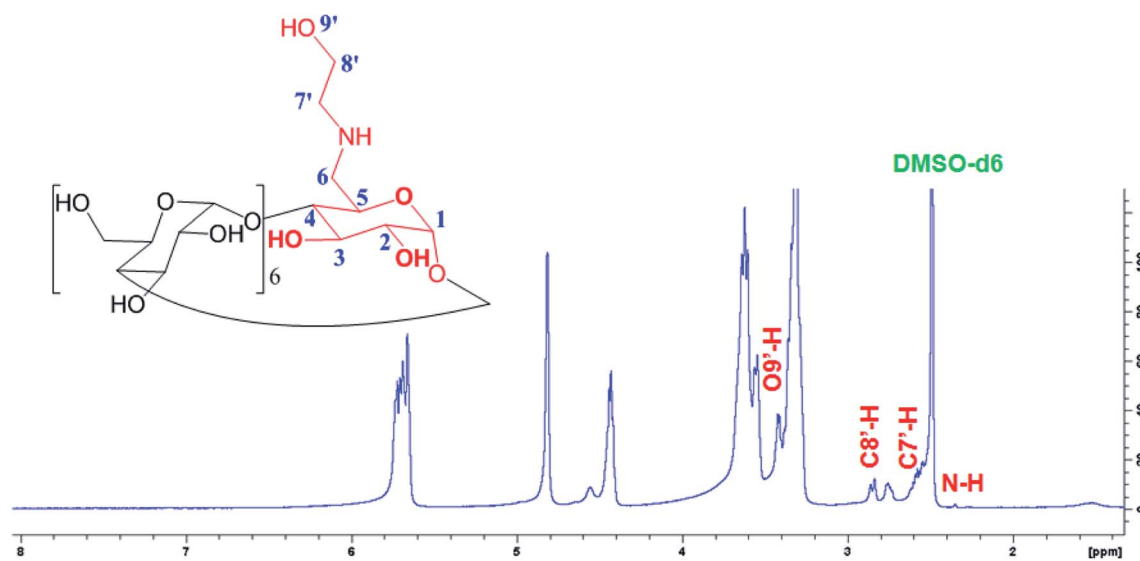


Fig. 2  $^1\text{H}$ -NMR spectrum of E- $\beta$ CD in the  $\text{d}_6$ -DMSO solvent.

The preparation of the two modified amino  $\beta$ CDs, mono-6-deoxy ethanolamine- $\beta$ CD (E- $\beta$ CD) and mono-6-deoxy diethylamine- $\beta$ CD (D- $\beta$ CD) were also confirmed using  $^1\text{H}$ -NMR and mass spectrometry (Fig. 1a and b). Positive mode HRMS (ESI) ( $[\text{M} - \text{H}]^+$ ) for E- $\beta$ CD ( $\text{C}_{44}\text{H}_{76}\text{NO}_{35}$ ) gives a calculated and found values of 1178.41924 and 1178.42008, respectively. The

calculated and found values for D- $\beta$ CD ( $\text{C}_{46}\text{H}_{80}\text{NO}_{34}$ ) in the HRMS (ESI) positive mode ( $[\text{M} - \text{H}]^+$ ) were 1190.45563 and 1190.45450, respectively.

Fig. 2 shows a new peaks of the proton signal appeared around 2.75 and 2.85 ppm belongs to the C8'-H and C7'-H proton, and other peaks at 2.0 and 3.35 ppm for N-H and O9'-H

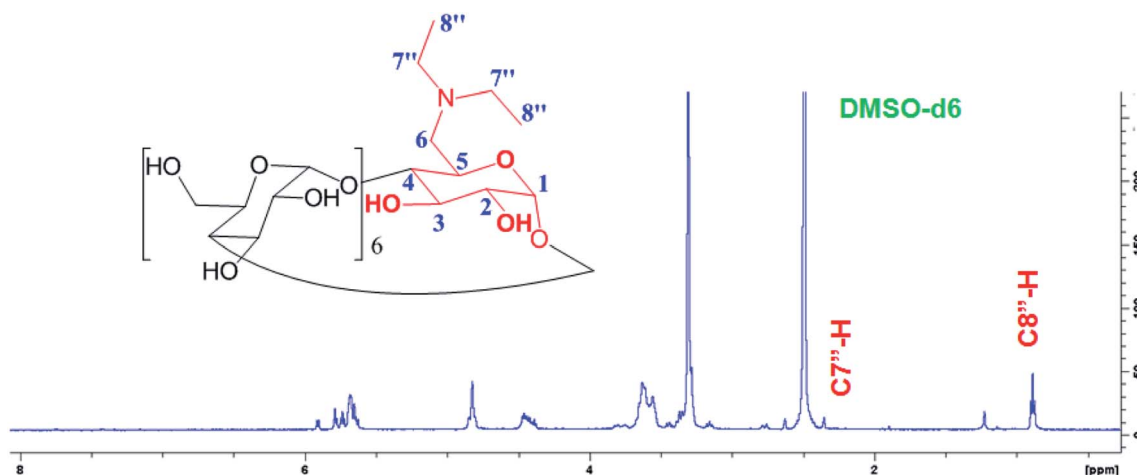


Fig. 3  $^1\text{H}$ -NMR spectrum of D- $\beta$ -CD in the  $d_6$ -DMSO solvent.

proton, respectively, of the ethanolamine substitution in E- $\beta$ -CD compared to  $^1\text{H}$ -NMR spectrum of  $\beta$ -CD (Fig. S5 $\dagger$ ).

$^1\text{H}$  NMR for E- $\beta$ -CD ( $d_6$ -DMSO,  $\delta$ , ppm): 2.01 (m, 1H, N-H), 3.35 (m, 1H, O'-H) 2.75 (d, 2H, H-8'), 2.85 (d, 2H, H-7'), 3.23–3.38 (m, 14H, H-2,4), 3.60–3.75 (m, 28H, H-3,5,6), 4.79 (d, 2H, H-1), 4.86 (t, 5H, H-1), 5.74 (m, 14H, OH-2,3).

New triplet peak of the proton signal appeared around 0.848 ppm belongs to the C8''-H proton of the methyl substituted in D- $\beta$ -CD in addition to the quartet peak around 2.450 ppm for the C7''-H (Fig. 3).

$^1\text{H}$  NMR for D- $\beta$ -CD ( $d_6$ -DMSO,  $\delta$ , ppm): 0.848 (m, 3H, H-8''), 2.45 (m, 2H, H-7''), 3.23–3.38 (m, 14H, H-2,4), 3.60–3.75 (m, 28H, H-3,5,6), 4.79 (d, 2H, H-1), 4.86 (t, 5H, H-1), 5.74 (m, 14H, OH-2,3).

### 3.2 Absorption spectra

Spectroscopy is one of the methods usually used to confirm inclusion complex formation.  $\beta$ -CD has no absorption in the range of 300–500 nm, while CRM has a maximum absorption at 420 nm (Fig. S7 $\dagger$ ), hence this wavelength was used for the study. The absorption spectra of CRM,  $\beta$ -CDs and their corresponding complexes were studied in accordance with the procedure mentioned above.

The effect of increasing the concentration of  $\beta$ -CDs (0.00–0.63 mM) on the absorption spectrum of CRM was studied with

a constant concentration of CRM (0.18 mM). As a result of the complexation, the chromophore, CRM, is transferred from the aqueous environment into the hydrophobic environment of the cyclodextrin's cavity. Hypsochromic or bathochromic shift, as well as increased absorption, are the commonly reported effects of the complex formation.<sup>38</sup>

Fig. S8 $\dagger$  shows a remarkable increase in CRM absorbance upon continuous addition of  $\beta$ -CD. This is maybe attributed to the transference of the two aromatic rings (chromophores) in CRM from the aqueous medium to the non-polar cavity of the  $\beta$ -CD. In addition, shielding of the excited species from non-radiative processes occurring in the bulk solution and may be due to the increase in the molar absorption coefficient of the inclusion complexes.<sup>39</sup> The same results were obtained for CRM absorption spectrum in the complexes formed with E- $\beta$ -CD and D- $\beta$ -CD as shown in Fig. S8b and c. $\dagger$

### 3.3 Determination of the complexation stoichiometry and formation constants

Continuous variation method (Job's method) was employed to determine the complexation stoichiometry. Job's plots are shown in Fig. 4, where the CRM mole fraction ( $\chi$ ) was varied from 0.0 to 1.0 and plotted against  $\chi$  multiplied with absorbance difference. As shown in Job's plot the maximum peak was

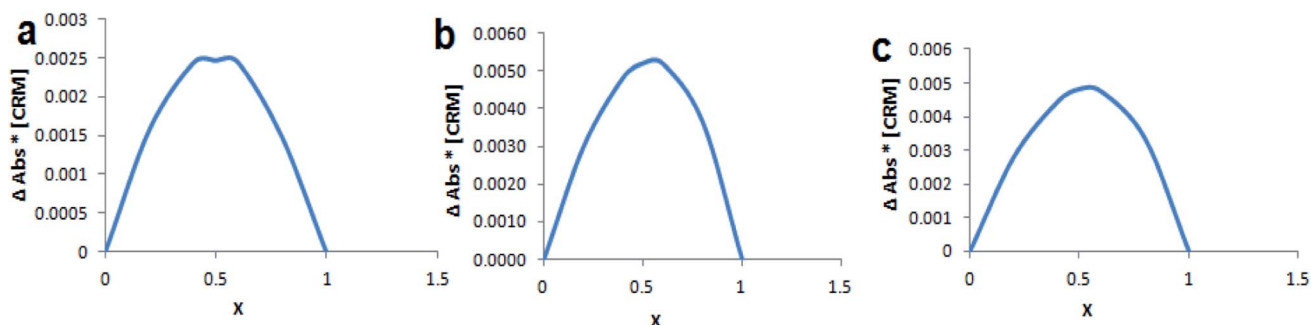


Fig. 4 Job's plot for (a) CRM- $\beta$ -CD, (b) CRM-D- $\beta$ -CD and (c) CRM-E- $\beta$ -CD, where  $x$  is the mole fraction of CRM.

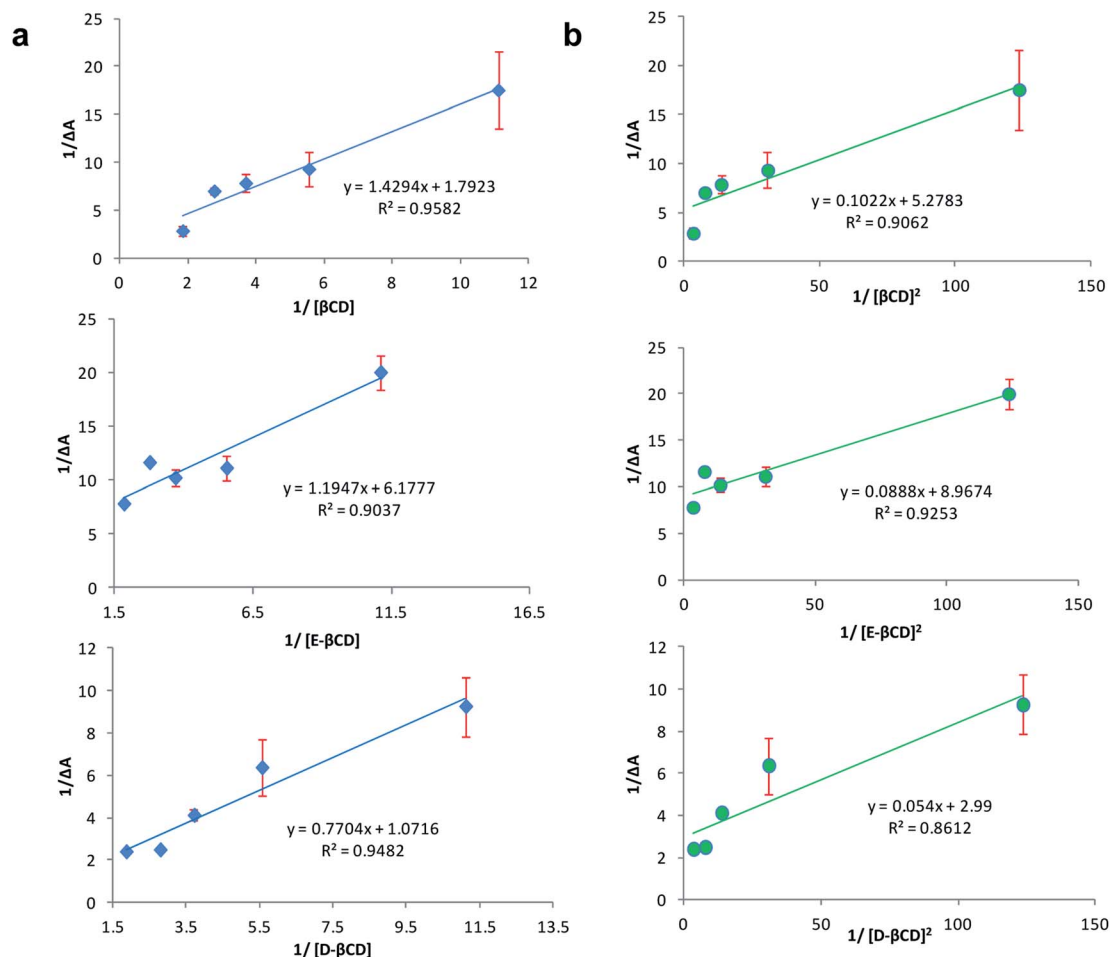


Fig. 5 Benesi–Hildebrand plot of (a)  $1/\Delta A$  versus  $1/[1/\beta CD]$  and (b)  $1/\Delta A$  versus  $1/[1/\beta CD]^2$  for CRM –  $\beta CD$  different complexes.

obtained at  $\chi = 0.5$ , which points to a 1 : 1 inclusion complex between CRM with native and modified  $\beta CD$ s.

The stoichiometry of the complexes was also determined using the Benesi–Hildebrand equations (Eqn (1) and (2)). A linear dependence of the type  $1/(A - A^0)$  vs.  $1/[CD]^n$ , with  $n = 1$  or 2, indicates the presence of complexes of 1 : 1 or 1 : 2 stoichiometry, respectively.<sup>32</sup> Fig. 5a and b represent the Benesi–Hildebrand plot of  $1/\Delta A$  versus  $1/[\beta CD]$  and  $1/[\beta CD]^2$  for native and modified CRM- $\beta CD$ . A good linear correlation was obtained for plotting  $1/\Delta A$  versus  $1/[\beta CD]$ , which indicates a 1 : 1 stoichiometry with a formation constant ( $K_f$ ) equal to 1.3, 5.2 and 1.4  $\text{mM}^{-1}$  for CRM- $\beta CD$ , CRM-E- $\beta CD$  and CRM-D- $\beta CD$  complexes, respectively. Another good linear correlation with a possibility of 1 : 2 stoichiometry appears from plotting of  $1/\Delta A$  versus  $1/[1/\beta CD]^2$  with a  $K_f$  of 51.6, 100.9 and 55.4  $\text{mM}^{-2}$  for CRM- $\beta CD$ , CRM-E- $\beta CD$ , and CRM-D- $\beta CD$  complexes, respectively. These result are consistent with Jahed *et al.* and Patro *et al.* conclusions of 1 : 1 or 1 : 2 stoichiometry based on phase solubility diagram, NMR results and molecular modelling calculations.<sup>40,41</sup> In addition, 1 : 2 ratio of CRM with hydroxyl propyl derivatives of  $\beta CD$  (HP- $\beta CD$ ) also strongly reported based on NMR studies.<sup>42</sup> Moreover, CRM forms strong 2 : 1 host : guest inclusion complexes with  $\beta CD$  and HP- $\beta CD$ , according to

Baglolo *et al.*, without eliminating the occurrence of 1 : 1 stoichiometry as confirmed by the fluorescence enhancement titration study of CRM upon complexation with increasing ratios of CDs.<sup>43</sup> Thus the formation of inclusion complexes with 1 : 2 (guest : host) stoichiometry is possible as well as the 1 : 1 complexes. The presence of the two stoichiometric possibilities may be due to solvent effects (buffer type) and CRM quality, but either ratios will not affect the spectrophotometric investigations of the inclusion complex.<sup>44</sup> Therefore, the 1 : 2 stoichiometry is more acceptable regarding higher formation constant and due to the large structure of CRM with two identical terminal aromatic rings that can be entrapped in two  $\beta CD$  molecules. The stoichiometric data show clearly that the modification on  $\beta CD$  did not affect its guest–host interaction modes with CRM, and hence can be used in remote loading into liposomes.

#### 3.4. Differential scanning calorimetry (DSC) and thermogravimetric analysis (TGA)

DSC method was used to determine the phase changes in the  $\beta CD$ s melting temperature due to the inclusion of CRM. Table S1† represents a summary of DSC endothermic peaks of CRM with various  $\beta CD$  complexes. CRM,  $\beta CD$ , E- $\beta CD$  and D- $\beta CD$

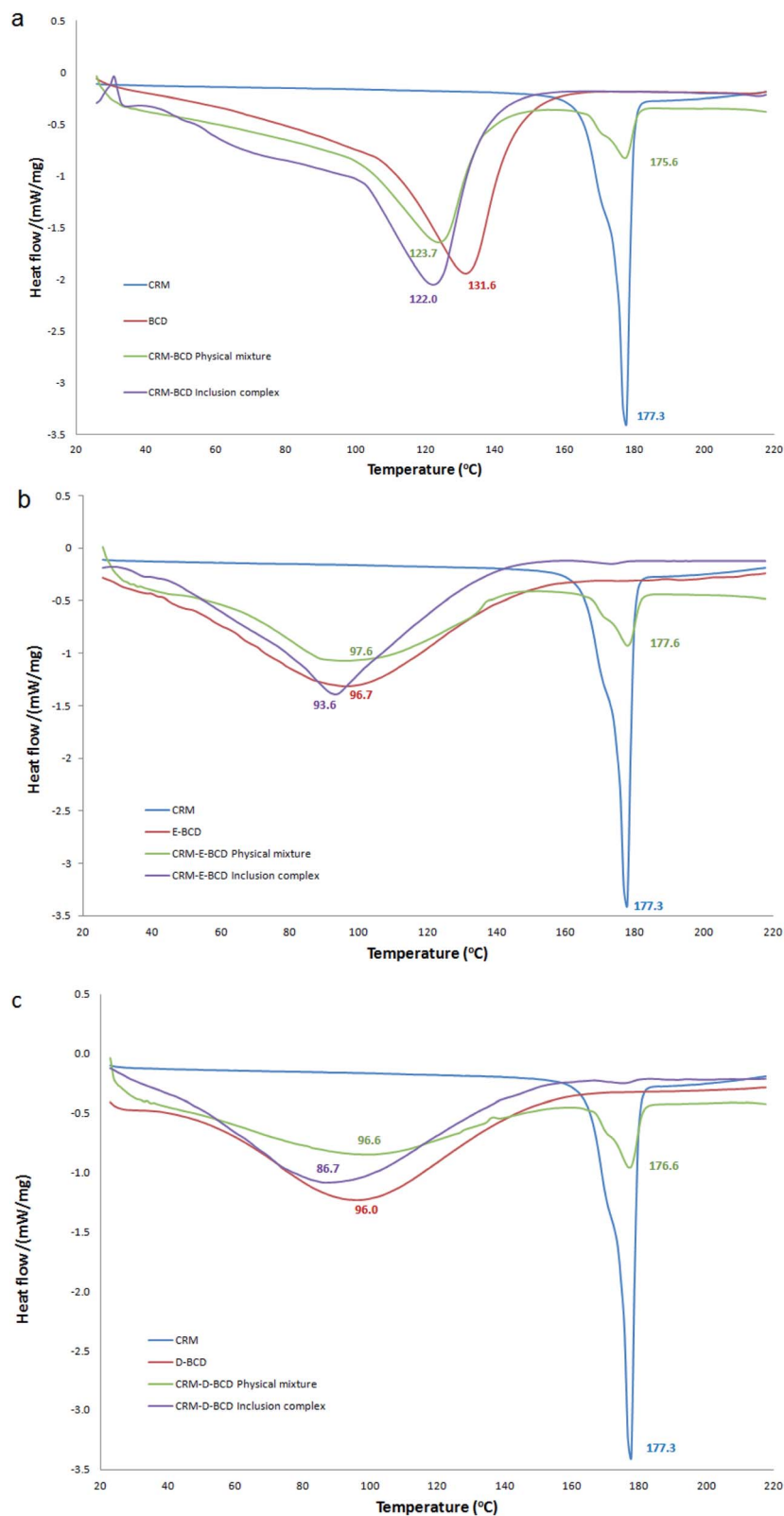


Fig. 6 DSC thermograms for (a) CRM- $\beta$ CD, (b) CRM-E- $\beta$ CD, and (c) CRM-D- $\beta$ CD compared to their precursors and physical mixtures.

have shown individual exothermic peaks at 177.3, 131.7, 96.6 and 96.0 °C, respectively, due to their melting points. DSC curves of CRM,  $\beta$ CDs, their physical mixture, and the inclusion

complex were shown in Fig. 6. The thermal profile of the physical mixture was actually a combination of characteristics of CRM and different  $\beta$ CDs without noticeable alteration in the



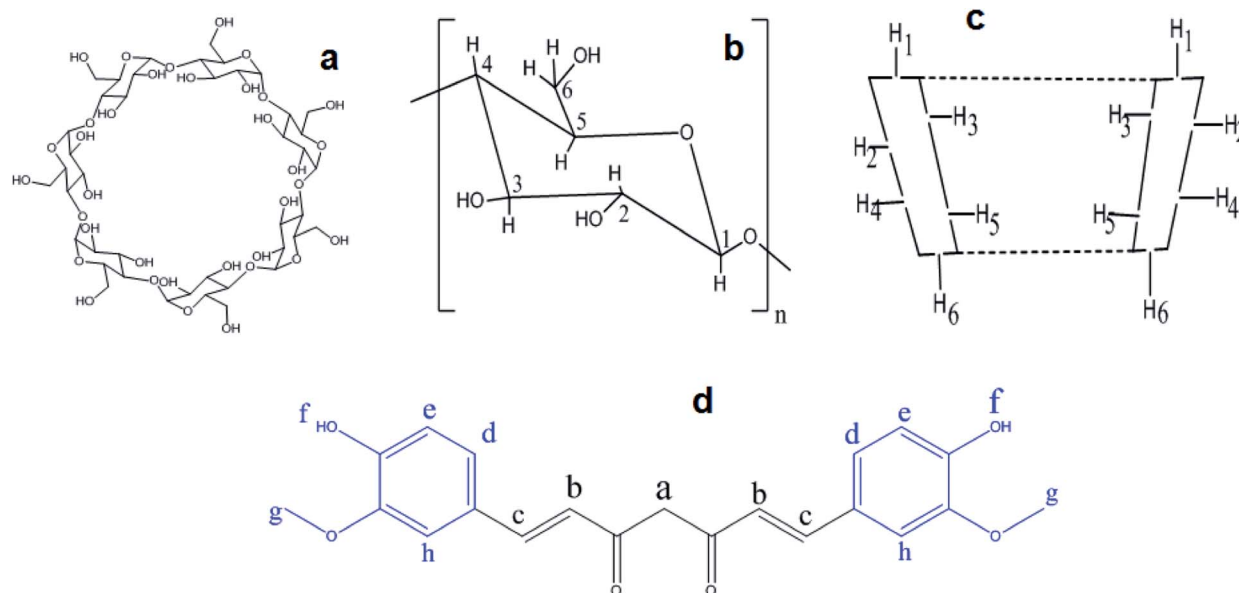


Fig. 7 The conformational structure  $\beta$ CD, (a and b). The major hydrogen atoms of  $\beta$ CD, (c). The chemical structure of curcumin, (d).

$\beta$ CDs endothermic peaks and CRM showed a sharp endothermic peak around 177.3. In contrast, the thermograms of CRM- $\beta$ CDs inclusion complexes did not show any peak of CRM in the 177.3 region and mainly showed features of  $\beta$ CDs with a decreasing in the melting points of CRM- $\beta$ CD, CRM-E- $\beta$ CD and CRM-D- $\beta$ CD to 122.0, 93.6 and 86.7, respectively. These data should confirm the formation of the inclusion complex and CRM molecules being included in the  $\beta$ CDs cavities by replacing water molecules, and this behavior is an indication of stronger interactions between CRM and  $\beta$ CDs in the solid-state.

The thermal stability of CRM- $\beta$ CD, CRM-E- $\beta$ CD and CRM-D- $\beta$ CD complexes were studied using TGA.<sup>45</sup> Fig. S9<sup>†</sup> shows the thermograms of the weight loss curves for CRM- $\beta$ CD, CRM-D- $\beta$ CD, CRM-E- $\beta$ CD and their precursors in the temperature range of 25–600 °C.  $\beta$ CD, D- $\beta$ CD, and E- $\beta$ CD start to decompose at 289, 261 and 224 °C, respectively. The chemical modification on  $\beta$ CD decrease the decomposition temperature of  $\beta$ CD. The thermal change occurred between 40 to 75 °C in different  $\beta$ CDs due to the endothermic behavior which corresponded to the loss of water molecules in  $\beta$ CDs cavities. CRM exhibited a major

weight loss at 230.3 °C. CRM inclusion complexes underwent weight loss in two major stages. The first stage is due to the dehydration of water molecules between 40 to 60 °C, while the second stage is due to decomposition of the complexes. Moreover, TGA thermograms (Fig. S9<sup>†</sup>) show a 63.5% weight loss and slight degradation of CRM at 600 °C and almost complete degradation with 91.02% weight loss for native  $\beta$ CD compared to the higher stability of modified  $\beta$ CD, E- $\beta$ CD and D- $\beta$ CD with 73.81 and 78.03% weight loss respectively, at 600 °C. In addition, the inclusion complexes enhance the thermal stability of CRM and decrease the weight loss of  $\beta$ CD, E- $\beta$ CD and D- $\beta$ CD to 78.34, 61.41 and 63.77%, respectively, which is probably due to the formation of CRM inclusion complexation with various  $\beta$ CDs.

### 3.5. <sup>1</sup>H-NMR spectroscopy

The complexation pattern was further evaluated by <sup>1</sup>H-NMR spectroscopy. This technique provides direct evidence of inclusion complex formation. Chemical shift ( $\delta$ ) changes, either for the host or the guest, can verify due to the formation of

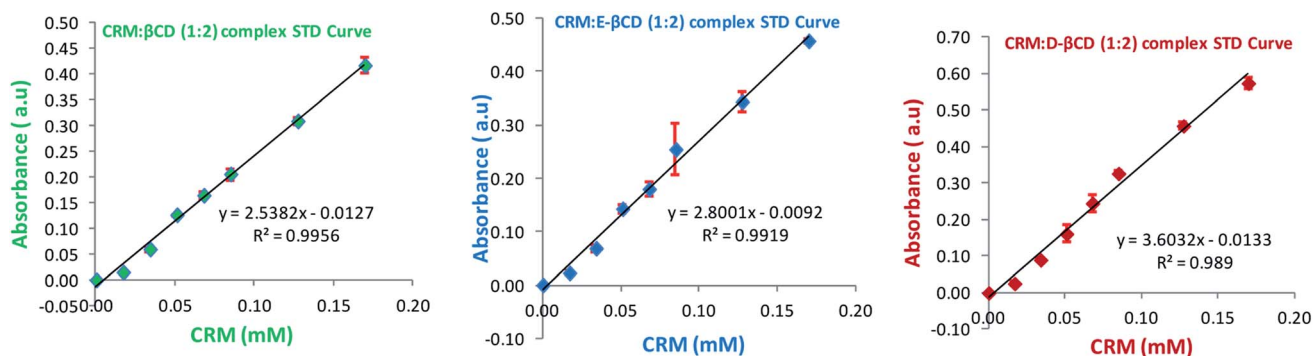


Fig. 8 Standard curves (STD) of different CRM- $\beta$ CD complexes.

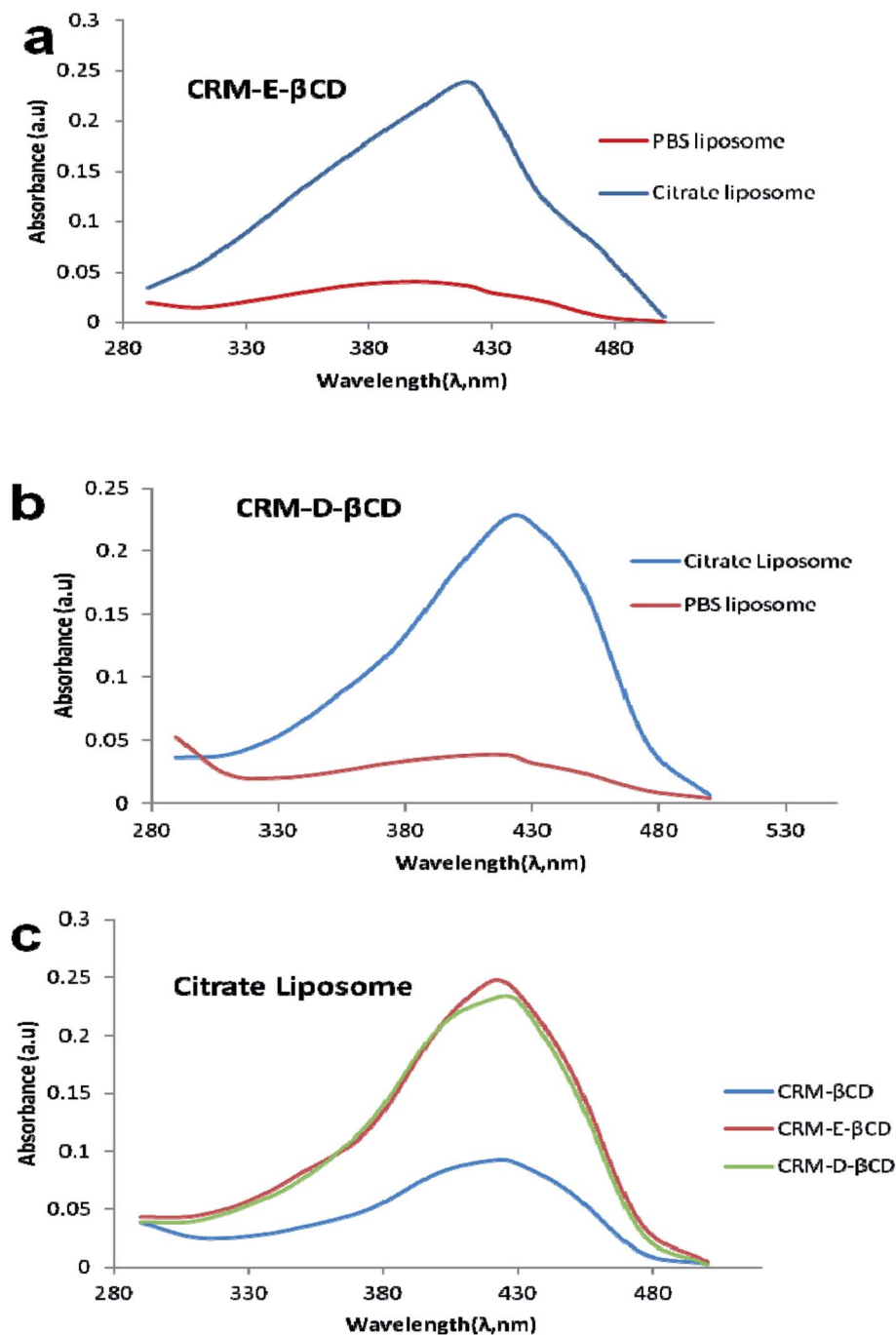


Fig. 9 Active loading of modified  $\beta$ -cyclodextrin using a transmembrane pH gradient. (a and b) represent the absorbance of CRM-E- $\beta$ CD and CRM-D- $\beta$ CD complexes, respectively, in absorption unit loaded into liposomes with a pH gradient (citrate liposomes) compared with that of the same complex loaded into liposomes in the absence of a pH gradient (PBS liposomes). (b) Absorbance of CRM- $\beta$ CD, CRM-E- $\beta$ CD and CRM-D- $\beta$ CD complex in absorption unit loaded into liposomes with a pH gradient (citrate liposomes).

inclusion complex in solution.<sup>11,46</sup> Fig. 7 represents the chemical structure of  $\beta$ CD and CRM with all hydrogen atoms that may be involved in complex formation. An overview of the complexation induced  $^1\text{H-NMR}$  chemical shifts of hydrogen atoms of free native, modified  $\beta$ CDs and CRM in  $d_6$ -DMSO compared to their respective complexes are presented in Tables S2–S4<sup>†</sup> and their corresponding detailed  $^1\text{H-NMR}$  spectrum are shown in Fig. S10–S12,<sup>†</sup> respectively. CRM has two terminal

aromatic rings that, theoretically, supposed to involve in the complex formation with the hydrophobic cavity of  $\beta$ CDs. The major shifts of  $\text{H}_d$  and  $\text{H}_g$  prove this hypothesis. In addition, CRM specific peaks between 6 and 7.5 ppm show low intensity and secondary hydroxyl proton,  $\text{H}_f$ , almost invisible which is a typical pattern of inclusion complexes.<sup>21</sup> Another noticeable chemical shift for CRM was for  $\text{H}_c$  which suggests the inclusion may go beyond the aromatic rings of CRM toward nearby atoms.

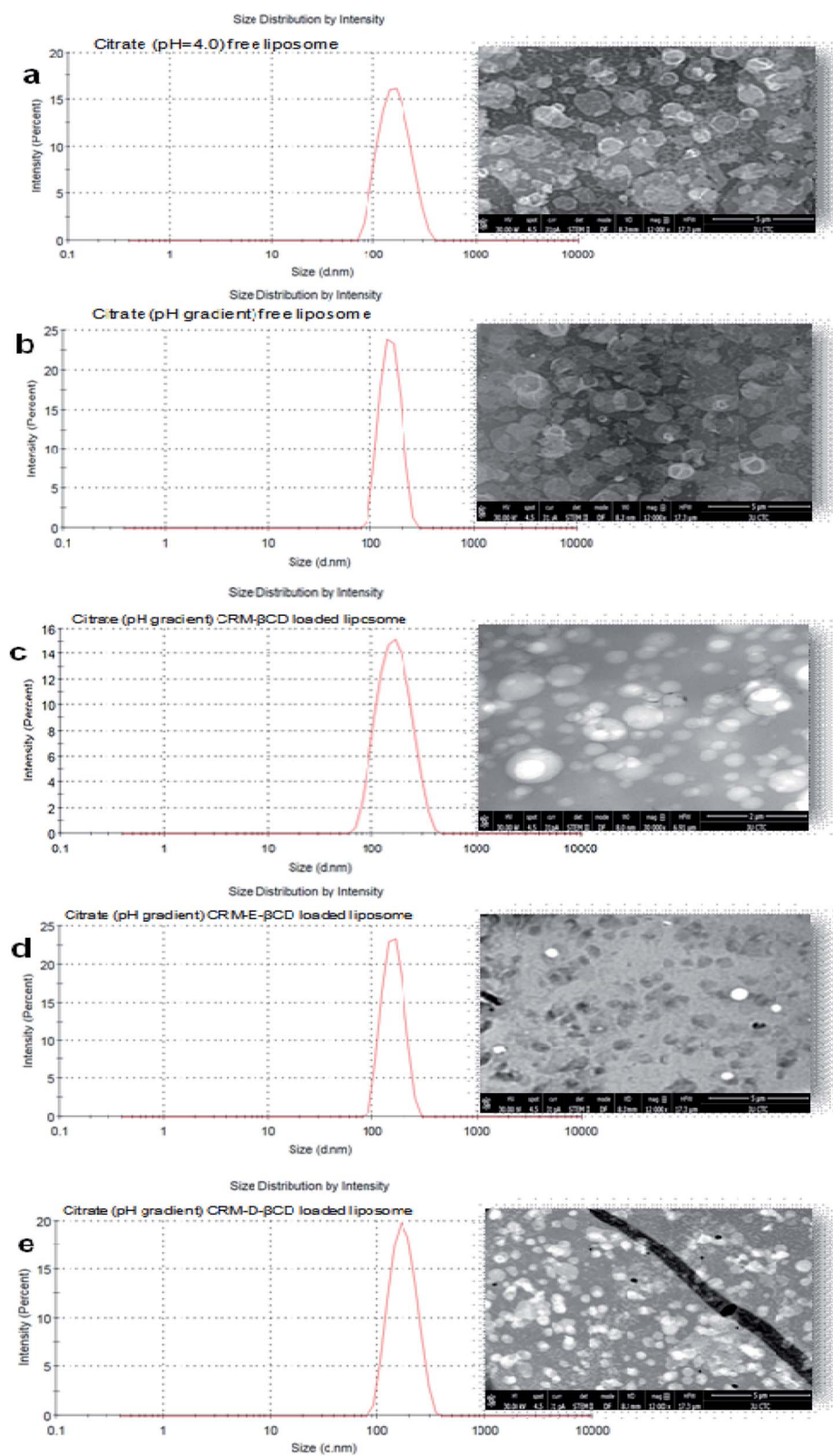


Fig. 10 Size distribution by DLS and TEM micrographs (a) pH = 4 blank liposomes, (b) pH gradient blank liposomes, (c) CRM-βCD loaded liposomes, (d) CRM-E-βCD loaded liposomes and (e) loaded CRM-D-βCD liposomes.

Table 1 Liposome characterization; average diameter, PDI, zeta potential and encapsulation efficiency. (mean  $\pm$  SD,  $n = 3$ )

Liposome	Complex type	Average particle size ( $Z_{avg}$ ) (d nm $\pm$ SD)	(PDI $\pm$ SD)	Zeta potential (mV $\pm$ SD)	(EE% $\pm$ SD)
PBS liposome	Free	139.39 $\pm$ 3.00	0.05 $\pm$ 0.04	-0.70 $\pm$ 2.94	—
	CRM-E- $\beta$ CD	146.13 $\pm$ 2.20	0.08 $\pm$ 0.01	-1.78 $\pm$ 2.60	10.74 $\pm$ 2.27
	CRM-D- $\beta$ CD	148.07 $\pm$ 2.49	0.09 $\pm$ 0.01	-4.74 $\pm$ 0.72	7.72 $\pm$ 2.33
Citrate liposome	Free	151.33 $\pm$ 2.03	0.04 $\pm$ 0.02	-7.00 $\pm$ 0.74	—
	CRM- $\beta$ CD	151.13 $\pm$ 1.42	0.03 $\pm$ 0.02	-8.93 $\pm$ 3.34	16.56 $\pm$ 7.38
	CRM-E- $\beta$ CD	152.40 $\pm$ 3.22	0.05 $\pm$ 0.02	-12.33 $\pm$ 0.21	51.16 $\pm$ 6.19
	CRM-D- $\beta$ CD	163.20 $\pm$ 1.05	0.04 $\pm$ 0.04	-18.07 $\pm$ 0.21	41.73 $\pm$ 1.53

The variation in the values of chemical shifts differences, and whether the shift occurs in the high or low field region, indicates the different types of  $\beta$ CD host.

Obvious chemical shifts for native and modified  $\beta$ CDs occurred at  $H_3$  and  $H_5$ , as expected since these atoms are located inside the cavity of the  $\beta$ CD, which confirms the formation of an inclusion complex.<sup>40</sup> A noticeable chemical shift in  $H_2$  and  $H_4$ , especially in the modified cyclodextrin, indicate the effect of these modified fragments (ethanol amine or diethyl amine) that located outside the cavity of  $\beta$ CD on the 6-position (easily rotate towered  $H_2$  and  $H_4$ ) on the chemical shifts of outside  $\beta$ CD protons. The large size of CRM may partially contact the outside protons of the nearby  $\beta$ CD and alter their chemical shifts. Cross-peaks observed in some cases also with the outside cyclodextrin proton  $H_4$  were ascribed to intramolecular scalar spin saturation transfers from the cyclodextrin protons  $H_3$  and/or  $H_5$ .<sup>47</sup> These observations may give evidence of the formation of partial or complete inclusion since  $H_5$  showed higher shifts than  $H_3$  for all complexes. All these data indicate the successful formation of inclusion complexes between CRM with native or modified  $\beta$ CD.

### 3.6. Liposome characterization and active loading

Following the chemical modifications of  $\beta$ CDs and the complexation with CRM, we have investigated the encapsulation of CRM into liposomes by active loading *via transmembrane* pH gradient. The liposomes were prepared by hydrating lipid films with 300 mM citrate buffer (pH 4), or with PBS (pH 7.4) for comparison. To achieve a pH gradient liposomes, the citrate liposomes were centrifuged and the liposomes pellets were then dispersed in 20 mM HEPES buffer (pH 10.5), then the CRM- $\beta$ CD complexes were incubated with the preformed liposomes at 65 °C for 1 h for entrapment.<sup>17</sup> The unloaded CRM complexes were removed by centrifugation followed by liposomes disruption to measure the encapsulation efficiency using UV spectroscopy (Fig. 8). Two types of control experiments were performed, the modified  $\beta$ CD complexes with PBS buffer liposome and native  $\beta$ CD with citrate pH gradient liposome.

In the absence of a pH gradient, there was little entrapment into the liposomes using native  $\beta$ CD complex as shown in Fig. 9. Dynamic light scattering experiments showed that free liposomes diameter was in the ranging 139.39–151.33 nm with

a narrow PDI (<0.10). Complex loading just slightly increased the diameter up to 163 nm, without affecting the PDI (Fig. 10). Table 1 represents liposome characteristics before and after active loading with different liposomes and CRM complexes. The zeta potential also varied among different formulations. The decreasing in zeta potential was due to the effect of external buffer and the capacity of modified amino  $\beta$ CD to alter phospholipids ionization.

TEM, the most frequently used imaging method for the evaluation of the structure of nanoparticles,<sup>11,48</sup> was employed to confirm the size and morphological characteristics of liposomes before and after active loading. TEM observations (Fig. 10) revealed that the liposomes were homogeneously formed in the intended formulation. The prepared liposomes almost maintained their spherical shape with uniformed dispersion and showed good stability in citrate buffer over the wide transmembrane pH gradient range. No noticeable changes or disruption were observed after liposomes active loading at 65 °C.<sup>49</sup>

Encapsulation efficiency is an expression of the amount of drug complex incorporated into the liposome and is normally defined as the percentage of drug complex entrapped in liposomes relative to the total amount of drug complex. Different factors affect the encapsulation efficiency such as pH gradient, aqueous media type, buffer concentration and the type of the ionized functional group.<sup>50</sup> We found that CRM-E- $\beta$ CD complex showed higher encapsulation efficiency in pH gradient liposomes compared to other formulation. E- $\beta$ CD, with its secondary amine, has a moderate  $pK_a$  that enables them to be in neutral form outside the liposome prior active loading. While in the case of D- $\beta$ CD, with its tertiary amine, the external 10.5 pH maybe not high enough to neutralize all the tertiary amino groups of D- $\beta$ CD, and some of them were protonated prior active loading which limited their active loading.

## 4. Conclusions

In conclusion, our results support the new active loading strategy for hydrophobic drugs into liposomes. This approach uses modified cyclodextrins with ionizable groups as a carrier and solubilizer. We have encapsulated a promising pharmaceutical agent, CRM, into the modified  $\beta$ CDs. The stoichiometry of 1 : 1 or 1 : 2 of the inclusion complex was determined by job's plot and modified Benesi-Hildebrand equation as well as the



formation constant of complexes. Entire complex characterization was also done, which confirms predominantly that the aromatic rings of the CRM have entrapped into the  $\beta$ CD cavity. This inclusion allowed CRM to be remotely loaded into liposomes and masking the undesirable characteristics of CRM with high encapsulation efficiency. Previous studies to incorporate CRM with liposomes were limited to passive loading. Passive loading often leads to undesirable membrane incorporation, lowering liposome stability, and is much less efficient than active loading. Since most promising drugs are hydrophobic, this strategy will enhance the solubility and the selectivity of drug delivery systems despite each drug requires a different approach to manage all of its properties. The type of cyclodextrin modification plays an important role in encapsulation efficiency in addition to the pH gradient range and the incubation temperature. This strategy opens the way for the entrapment of various hydrophobic drugs into the biocompatible liposomes with high entrapment efficiency. Our study brings the idea to support the use of  $\beta$ CDs as a key tool to improve CRM characteristics for using this widely available natural product into effective drugs. Other forms of cyclodextrins, as  $\gamma$ -CD, have a pocket of larger size, can be used to encapsulate larger or additional compounds.

## Conflicts of interest

The authors declare no conflict of interest.

## References

- 1 T. Loftsson, S. B. Vogensen, M. E. Brewster and F. Konradsdottir, *J. Pharm. Sci.*, 2007, **96**(10), 2532–2546.
- 2 J. W. Park, *Breast Cancer Res.*, 2002, **4**(3), 95–99.
- 3 S. S. Dhule, P. Penfornis, T. Frazier, R. Walker, J. Feldman, G. Tan, J. He, A. Alb, V. John and R. Pochampally, *Nanomedicine*, 2012, **8**(4), 440–451.
- 4 G. T. Noble, J. F. Stefanick, J. D. Ashley, T. Kiziltepe and B. Bilgicer, *Trends Biotechnol.*, 2014, **32**(1), 32–45.
- 5 A. Hafner, J. Lovric, G. P. Lakos and I. Pepic, *Int. J. Nanomed.*, 2014, **9**, 1005–1023.
- 6 J. Gubernator, *Expert Opin. Drug Delivery*, 2011, **8**(5), 565–580.
- 7 S. H. Hwang, Y. Maitani, X. R. Qi, K. Takayama and T. Nagai, *Int. J. Pharm.*, 1999, **179**(1), 85–95.
- 8 A. Ascenso, M. Cruz, C. Euleterio, F. A. Carvalho, N. C. Santos, H. C. Marques and S. Simoes, *J. Liposome Res.*, 2013, **23**(3), 211–219.
- 9 Y. Deng, J. Ling and M. H. Li, *Nanoscale*, 2018, **10**(15), 6781–6800.
- 10 T. M. Allen and P. R. Cullis, *Adv. Drug Delivery Rev.*, 2013, **65**(1), 36–48.
- 11 W. Alshaer, M. Zraikat, A. Amer, H. Nsairat, Z. Lafi, D. A. Alqudah, E. Al Qadi, T. Alsheleh, F. Odeh, A. Alkaraki, M. Zihlif, Y. Bustanji, E. Fattal and A. Awidi, *RSC Adv.*, 2019, **9**(53), 30976–30988.
- 12 X. Zhang and C. Wang, *Chem. Soc. Rev.*, 2011, **40**(1), 94–101.
- 13 E. M. M. Del Valle, *Process Biochem.*, 2004, **39**(9), 1033–1046.
- 14 T. R. Thatiparti and H. A. von Recum, *Macromol. Biosci.*, 2010, **10**(1), 82–90.
- 15 G. Astray, C. Gonzalez-Barreiro, J. C. Mejuto, R. Rial-Otero and J. Simal-Gándara, *Food Hydrocolloids*, 2009, **23**(7), 1631–1640.
- 16 P. Purkayastha, S. S. Jaffer and P. Ghosh, *Phys. Chem. Chem. Phys.*, 2012, **14**(16), 5339–5348.
- 17 S. Sur, A. C. Fries, K. W. Kinzler, S. Zhou and B. Vogelstein, *Proc. Natl. Acad. Sci. U. S. A.*, 2014, **111**(6), 2283–2288.
- 18 D. B. Fenske and P. R. Cullis, *Expert Opin. Drug Delivery*, 2008, **5**(1), 25–44.
- 19 D. C. Drummond, C. O. Noble, Z. Guo, K. Hong, J. W. Park and D. B. Kirpotin, *Cancer Res.*, 2006, **66**(6), 3271–3277.
- 20 G. Bar-Sela, R. Epelbaum and M. Schaffer, *Curr. Med. Chem.*, 2010, **17**(3), 190–197.
- 21 M. M. Yallapu, M. Jaggi and S. C. Chauhan, *Colloids Surf., B*, 2010, **79**(1), 113–125.
- 22 T. L. Lapenda, W. A. Morais, F. J. Almeida, M. S. Ferraz, M. C. Lira, N. P. Santos, M. A. Maciel and N. S. Santos-Magalhaes, *J. Biomed. Nanotechnol.*, 2013, **9**(3), 499–510.
- 23 H. Arima, Y. Hagiwara, F. Hirayama and K. Uekama, *J. Drug Targeting*, 2006, **14**(4), 225–232.
- 24 N. Wang, X. Yu, K. Zhang, C. A. Mirkin and J. Li, *J. Am. Chem. Soc.*, 2017, **139**(36), 12354–12357.
- 25 H.-M. Shen and H.-B. Ji, *Carbohydr. Res.*, 2012, **354**, 49–58.
- 26 M. M. Yallapu, M. Jaggi and S. C. Chauhan, *Colloids Surf., B*, 2010, **79**(1), 113–125.
- 27 H. Y. Wang, J. Han and X. G. Feng, *Spectrochim. Acta, Part A*, 2007, **66**(3), 578–585.
- 28 J. S. Negi and S. Singh, *Carbohydr. Polym.*, 2013, **92**(2), 1835–1843.
- 29 C. Nicolazzi, S. Abdou, J. Collomb, A. Marsura and C. Finance, *Bioorg. Med. Chem.*, 2001, **9**(2), 275–282.
- 30 T. Cardoso, C. I. C. Galhano, M. F. Ferreira Marques and A. Moreira da Silva, *Spectros. Int. J.*, 2012, **27**(5–6), 329–336.
- 31 R. Rajaram, K. N. Sundararajulu and S. Meenakshisundaram, *J. Fluoresc.*, 2011, **21**(2), 521–529.
- 32 C. Tablet, I. Matei and M. Hillebrand, *The Determination of the Stoichiometry of Cyclodextrin Inclusion Complexes by Spectral Methods: Possibilities and Limitations*, INTECH Open Access Publisher, 2012.
- 33 K. Srinivasan, T. Stalin and K. Sivakumar, *Spectrochim. Acta, Part A*, 2012, **94**, 89–100.
- 34 F. Odeh, S. I. Ismail, R. Abu-Dahab, I. S. Mahmoud and A. Al Bawab, *Drug Delivery*, 2012, **19**(8), 371–377.
- 35 A. D. Bangham, M. M. Standish and J. C. Watkins, *J. Mol. Biol.*, 1965, **13**(1), 238–252.
- 36 S. G. M. Ong, L. C. Ming, K. S. Lee and K. H. Yuen, *Pharmaceutics*, 2016, **8**(3), 25.
- 37 P. Panwar, B. Pandey, P. C. Lakhera and K. P. Singh, *Int. J. Nanomed.*, 2010, **5**, 101–108.
- 38 S. Hashimoto and J. K. Thomas, *J. Am. Chem. Soc.*, 1985, **107**(16), 4655–4662.
- 39 S. Mohamad, H. Surikumaran, M. Raoov, T. Marimuthu, K. Chandrasekaram and P. Subramaniam, *Int. J. Mol. Sci.*, 2011, **12**(9), 6329–6345.



- 40 V. Jahed, A. Zarrabi, A.-k. Bordbar and M. S. Hafezi, *Food Chem.*, 2014, **165**, 241–246.
- 41 N. M. Patro, A. Sultana, K. Terao, D. Nakata, A. Jo, A. Urano, Y. Ishida, R. N. Gorantla, V. Pandit, K. Devi, S. Rohit, B. K. Grewal, E. M. Sophia, A. Suresh, V. K. Ekbote and S. Suresh, *J. Inclusion Phenom. Macrocyclic Chem.*, 2014, **78**(1–4), 471–483.
- 42 Z. Aytac and T. Uyar, *Int. J. Pharm.*, 2017, **518**(1), 177–184.
- 43 K. N. Baglole, P. G. Boland and B. D. Wagner, *J. Photochem. Photobiol., A*, 2005, **173**(3), 230–237.
- 44 A. B. Hegge, M. Masson, S. Kristensen and H. H. Tonnesen, *Pharmazie*, 2009, **64**(6), 382–389.
- 45 K. P. Sambasevam, S. Mohamad, N. M. Sarih and N. A. Ismail, *Int. J. Mol. Sci.*, 2013, **14**(2), 3671–3682.
- 46 B. Cwiertnia, T. Hladon and M. Stobiecki, *J. Pharm. Pharmacol.*, 1999, **51**(11), 1213–1218.
- 47 H.-J. Schneider, F. Hacket, V. Rüdiger and H. Ikeda, *Chem. Rev.*, 1998, **98**(5), 1755–1786.
- 48 J. Kuntsche, J. C. Horst and H. Bunjes, *Int. J. Pharm.*, 2011, **417**(1–2), 120–137.
- 49 M. Placzek and M. Kosela, *Acta Pharm.*, 2016, **66**(1), 1–22.
- 50 S. Du and Y. Deng, *Drug Dev. Ind. Pharm.*, 2006, **32**(7), 791–797.